Electronic supplementary information (ESI)

New Journal of Chemistry

Modulating the structural topologies and magnetic relaxation behaviour of the Mn-Dy compounds through employing different auxiliary organic ligands

Hui-Sheng Wang,*[a] Yong Chen,[a] Zhao-Bo Hu,[b] Ke Zhang,[a] Zaichao Zhang,[c] You Song*[b] and Zhi-Quan Pan[a]

[a] School of Chemistry and Environmental Engineering, Key Laboratory of Green Chemical Process of Ministry of Education, Key Laboratory of Novel Reactor and Green Chemical Technology of Hubei Province, Wuhan Institute of Technology, Wuhan 430074, P. R. China.

[b] State Key Laboratory of Coordination Chemistry, School of Chemistry and Chemical Engineering, Collaborative Innovation Center of Advanced Microstructures, Nanjing University, Nanjing 210046, P. R. China.

[c] Jiangsu Key Laboratory for the Chemistry of Low-dimensional Materials, College of Chemistry and Chemical Engineering, Huaiyin Normal University, Huai'an 223300, P. R. China.

Corresponding author, E-mail: wangch198201@163.com (H.-S.W.); yousong@nju.edu.cn (Y. S.)

Table S1. Crystal data and structure refinement parameters for **1** and **2**.

Compounds	**1**	**2**
Formula	$C_{62}H_{61}Cl_2DyMn_4N_8O_{17}$	$C_{72}H_{86}Mn_4Dy_2N_{14}O_{27}$
Formula weight	1643.34	2124.30
Crystal colour	brown	light brown
Crystal size/mm	0.32 × 0.08 × 0.07	0.13 × 0.11 × 0.07
Crystal system	monoclinic	monoclinic
Space group	*C*2/*c*	*C*2/*c*
a (Å)	25.1051(11)	18.7726(14)
b (Å)	26.7821(9)	11.0470(7)
c (Å)	22.7889(10)	19.4765(13)
α (°)	90	90
β (°)	100.298(2)	97.954(2)
γ (°)	90	90
Unit cell volume ($Å^3$)	15075.7(11)	4000.2(5)
Temperature (K)	173(2)	173(2)
Z	8	2
Wavelength (Å)	0.71073	0.71073
μ (Mo Kα) [mm^{-1}]	1.767	2.546
D_c (g cm^{-3})	1.448	1.764
θ *range* (°)	3.0674-25.3726	2.9019-25.2760
Index ranges	$-29 \le h \le 26$ $-31 \le k \le 31$ $-27 \le l \le 27$	$-22 \le h \le 22$ $-13 \le k \le 13$ $-23 \le l \le 21$
F(000)	6600	2128
Reflections collected	75457	12268
Unique reflections [R_{int}]	13053	3512
Reflections with $I > 2\sigma(I)$	9604	2836
Final *R* indices ($I > 2\sigma(I)$) [a,b]	$R_1 = 0.0952$, $wR_2 = 0.2016$	$R_1 = 0.0390$, $wR_2 = 0.0719$
Final *R* indices (all data)	$R_1 = 0.01341$, $wR_2 = 0.2157$	$R_1 = 0.0592$, $wR_2 = 0.0763$
S (all data)	1.096	1.046
$(\Delta\rho)_{max,min}$/e $Å^{-3}$	3.449 and -3.550	0.930 and -0.758

[a] $R_1 = \Sigma(||F_o| - |F_c||)/\Sigma|F_o|$. [b] $wR_2 = [\Sigma[w(F_o^2 - F_c^2)^2]/\Sigma[w(F_o^2)^2]]^{1/2}$, $w = 1/[\sigma^2(F_o^2) + [(ap)^2 + bp]$, where $p = [\max(F_o^2, 0) + 2F_c^2]/3$.

Table S2. Selected bond lengths (Å) and angles (°) for **1**.

Selected bond lengths for **1**					
Cl1-Mn4	2.667(4)	Dy1-O5	2.415(7)	Mn3-O9	1.869(8)
Cl1-Mn1	2.687(4)	Mn1-O1	1.870(9)	Mn3-O10	1.888(8)
Cl2-Mn2	2.686(4)	Mn1-O2	1.891(8)	Mn3-O12	1.958(7)
Cl2-Mn3	2.642(4)	Mn1-O4	1.937(7)	Mn3-N5	1.970(10)
Dy1-O10	2.314(8)	Mn1-N1	1.981(10)	Mn3-N6	2.270(10)
Dy1-O15	2.346(8)	Mn1-N2	2.298(11)	Mn4-O15	1.876(8)
Dy1-O12	2.348(8)	Mn2-O6	1.878(8)	Mn4-O14	1.875(9)
Dy1-O7	2.357(8)	Mn2-O7	1.878(8)	Mn4-O13	1.979(8)
Dy1-O4	2.365(8)	Mn2-O5	1.939(8)	Mn4-N8	1.983(10)
Dy1-O2	2.369(8)	Mn2-N4	1.966(10)	Mn4-N7	2.260(10)
Dy1-O13	2.402(8)	Mn2-N3	2.307(11)		
Selected bond angles for 1					
O2-Dy1-O13	82.2(3)	O2-Mn1-O4	86.6(4)	O10-Mn3-O12	84.5(3)
O15-Dy1-O4	85.5(3)	O4-Mn1-N1	167.7(4)	O10-Mn3-N5	83.3(4)
O12-Dy1-O4	172.9(3)	N1-Mn1-N2	96.0(4)	O9-Mn3-O12	99.8(3)
O15-Dy1-O12	91.9(3)	O1-Mn1-Cl1	94.3(3)	O12-Mn3-N5	165.9(4)
O10-Dy1-O7	110.1(3)	N2-Mn1-Cl1	171.0(3)	N5-Mn3-N6	97.4(4)
O15-Dy1-O7	72.3(3)	O6-Mn2-O7	175.2(4)	O9-Mn3-Cl2	89.7(3)
O4-Dy1-O5	56.9(2)	O6-Mn2-O5	99.2(4)	N6-Mn3-Cl2	169.9(3)
O2-Dy1-O5	95.2(3)	O5-Mn2-N4	168.3(4)	O15-Mn4-O14	172.9(4)
O7-Dy1-O2	158.3(3)	O6-Mn2-N4	92.4(4)	O14-Mn4-O13	102.5(4)
O4-Dy1-O2	67.4(3)	N4-Mn2-N3	105.7(4)	O13-Mn4-N8	166.5(4)
O7-Dy1-O13	117.9(3)	O6-Mn2-Cl2	91.3(3)	N8-Mn4-N7	102.7(4)
O1-Mn1-O2	176.2(4)	N4-Mn2-Cl2	87.0(3)	O15-Mn4-Cl1	85.2(3)
O1-Mn1-O4	96.8(4)	O9-Mn3-O10	174.9(3)	N7-Mn4-Cl1	168.3(3)

Table S3. Selected bond lengths (Å) and angles (°) for **2**.

Selected bond lengths for **2**					
Dy1-O5	2.285(3)	Dy1-O5[a]	2.285(3)	Dy1-O4	2.339(3)
Dy1-O4[a]	2.339(3)	Dy1-O2	2.351(3)	Dy1-O2[a]	2.351(3)
Dy1-N2	2.574(4)	Dy1-N2[a]	2.574(4)	Mn1-O1	1.879(3)
Mn1-O4	1.894(3)	Mn1-O2	1.896(3)	Mn1-N1	1.970(4)
Mn1-N3	2.292(4)	Mn1-O3	2.310(3)		

Selected bond angles for **2**					
O5-Dy1-O5a	87.06(19)	O5-Dy1-O4	84.72(12)	O5-Dy1-O4	143.05(12)
O5-Dy1-O4a	84.72(12)	O4-Dy1-O4a	121.63(15)	O5- Dy1- O2	151.12(12)
O5- Dy1- O2a	90.45(12)	O4- Dy1- O2	80.10(11)	O4- Dy1- O2a	65.02(10)
O2- Dy1- O2a	104.92(15)	O5- Dy1- N2	78.59(13)	O5- Dy1- N2a	77.90(12)
O4- Dy1- N2	134.84(11)	O4- Dy1- N2a	64.47(11)	O2- Dy1- N2	128.90(11)
O2- Dy1- N2a	73.41(11)	O5- Dy1- N2	77.89(12)	O5- Dy1- N2a	78.59(13)
O4- Dy1- N2	64.47(11)	O4- Dy1- N2	134.84(11)	O2- Dy1- N2	73.41(11)
O2- Dy1- N2a	128.90(11)	N2- Dy1- N2a	147.35(17)	O1- Mn1- O4	101.02(13)
O1- Mn1- O2	175.48(13)	O4- Mn1- O2	83.35(13)	O1- Mn1- N1	92.25(15)
O4- Mn1- N1	165.68(15)	O2- Mn1- N1	83.52(14)	O1- Mn1- N3	87.60(16)
O4- Mn1- N3	94.20(15)	O2- Mn1- N3	90.93(16)	N1- Mn1- N3	91.71(16)
O1- Mn1- O3	89.22(13)	O4- Mn1- O3	86.70(13)	N1- Mn1- O3	88.12(14)

Symmetry code: a 0.5+x, -0.5-y, -0.5+z

Table S4. Bond valence sum (BVS) calculations for determining of the protonation levels of the O atoms in **1**

Atoms in **1**	BVS values of **1**	Atoms in **1**	BVS values of in **1**
O1	1.95	O2	1.99
O3	0.97	O4	2.01
O5	1.94	O6	1.88
O7	2.01	O8	0.87
O9	1.95	O10	2.11
O11	0.85	O12	1.96
O13	1.81	O14	1.88
O15	2.05	O16	0.94

The values of BVS calculations for O atoms in the ~1.8–2.0, ~1.0–1.2, and ~0.2–0.4 ranges are indicative of non-, single- and double-protonation, respectively. Single protonated alkoxido-type O atoms on the organic ligands were labelled using red.

Table S5. Bond valence sum (BVS) calculations for determining of the protonation levels of the O atoms in **2**.

Atoms in **2**	BVS values of **2**	Atoms in **2**	BVS values of in **2**
O1	1.92	O2	2.02
O3	1.13	O4	2.11
O5	1.92	O6	1.45

The values of BVS calculations for O atoms in the ~1.8–2.0, ~1.0–1.2, and ~0.2–0.4 ranges are indicative of non-, single- and double-protonation, respectively. Single protonated alkoxido-type O atoms on the organic ligands were labelled using red.

Table S6. Bond valence sum (BVS) calculations for determining of the oxidation states of the Mn atoms in **1**

Mn atom in complex **1**	Mn(II)	Mn(III)	Mn(IV)
Mn (1)	3.05	<u>3.24</u>	3.18
Mn (2)	3.52	<u>3.27</u>	3.22
Mn (3)	3.54	<u>3.28</u>	3.22
Mn (4)	3.49	<u>3.23</u>	3.19

The values labeled by underline indicated that they are close to the assigned oxidation state of Mn atoms. In **1**, the oxidation states of four Mn atoms are all +3.

Table S7. Bond valence sum (BVS) calculations for determining of the oxidation states of the Mn atoms in **2**.

Mn atom in complex **2**	Mn(II)	Mn (III)	Mn (IV)
Mn(1)	3.62	<u>3.42</u>	3.37

The values labeled by underline indicated that they are close to the assigned oxidation state of Mn atoms. In **2**, the oxidation state of Mn atom is +3.

Table S8. The possible geometries of nona-coordination metal centers and Deviation parameters from each ideal polyhedron for Dy of complex **1**.

Point group	Geometry	Polyhedron	Dy1
D_{8h}	OP-8	Octagon	31.809
C_{7v}	HPY-8	Heptagonal pyramid	24.231
D_{6h}	HBPY-8	Hexagonal bipyramid	8.857
O_h	CU-8	Cube	2.654
D_{4d}	SAPR-8	Square antiprism	5.448
D_{2d}	TDD-8	Triangular dodecahedron	4.456
D_{2d}	JGBF-8	Johnson - Gyrobifastigium (J26)	15.980
D_{3h}	JETBPY-8	Johnson - Elongated triangular bipyramid (J14)	22.204
C_{2v}	JBTP-8	Johnson - Biaugmented trigonal prism (J50)	7.635

C_{2v}	BTPR-8	Biaugmented trigonal prism	6.827
D_{2d}	JSD-8	Snub disphenoid (J84)	9.299
T_d	TT-8	Triakis tetrahedron	3.525
D_{3h}	ETBPY-8	Elongated trigonal bipyramid	19.937

Table S9. The possible geometries of oct-coordination metal centers and Deviation parameters from each ideal polyhedron for Dy of complex **2**.

Point group	Geometry	Polyhedron	Dy1
D_{8h}	OP-8	Octagon	31.114,
C_{7v}	HPY-8	Heptagonal pyramid	23.918
D_{6h}	HBPY-8	Hexagonal bipyramid	15.780
O_h	CU-8	Cube	13.347
D_{4d}	SAPR-8	Square antiprism	4.304
D_{2d}	TDD-8	Triangular dodecahedron	2.363
D_{2d}	JGBF-8	Johnson-Gyrobifastigium (J26)	11.826
D_{3h}	JETBPY-8	Johnson-Elongated triangular bipyramid (J14)	24.272
C_{2v}	JBTP-8	Johnson - Biaugmented trigonal prism (J50)	2.169
C_{2v}	BTPR-8	Biaugmented trigonal prism	2.375
D_{2d}	JSD-8	Snub disphenoid (J84)	3.057
T_d	TT-8	Triakis tetrahedron	13.612
D_{3h}	ETBPY-8	Elongated trigonal bipyramid	22.743

Table S10. The obtained parameters of τ_0 and U_{eff} for **1** by employing the equation $\ln(\chi''/\chi') = \ln(\omega\tau_0) + U_{eff}/k_BT$.

Frequencies	τ_0	U_{eff}	Frequencies	τ_0	U_{eff}
45 Hz	7.89×10^{-5}	8.14 K	251 Hz	4.55×10^{-4}	7.66 K
63 Hz	9.40×10^{-5}	8.59 K	355 Hz	5.59×10^{-4}	7.69 K
89 Hz	1.74×10^{-4}	8.01 K	500 Hz	7.30×10^{-4}	7.57 K
125 Hz	2.31×10^{-4}	8.02 K	707 Hz	8.53×10^{-4}	7.69 K
177 Hz	3.47×10^{-4}	7.74 K	999 Hz	1.14×10^{-3}	7.45 K
Mean value of τ_0			4.67×10^{-4}		
Mean value of U_{eff}			7.9 K		

Table S11. Best fitted parameters obtained for the extended Debye model with ac susceptibility data from SQUID magnetometer of compound **2** in the 1500 Oe applied field.

	T(K)	χ_S	χ_T	τ (s)	α	Residual
1	1.8	0.10519	0.709	5.41496E-4	0.22744	9.48617E-4
2	2.1	0.10789	0.65227	2.27528E-4	0.19111	6.51278E-4

3	2.4	0.00929	0.62469	6.30853E-5	0.25501	3.87345E-4
4	2.7	3.44032E-8	0.59006	2.46062E-5	0.25873	1.13373E-4
5	3.0	5.45275E-8	0.55544	8.97329E-6	0.29269	1.13031E-4
6	3.3	7.69405E-8	0.52566	3.19055E-6	0.33194	3.10198E-5

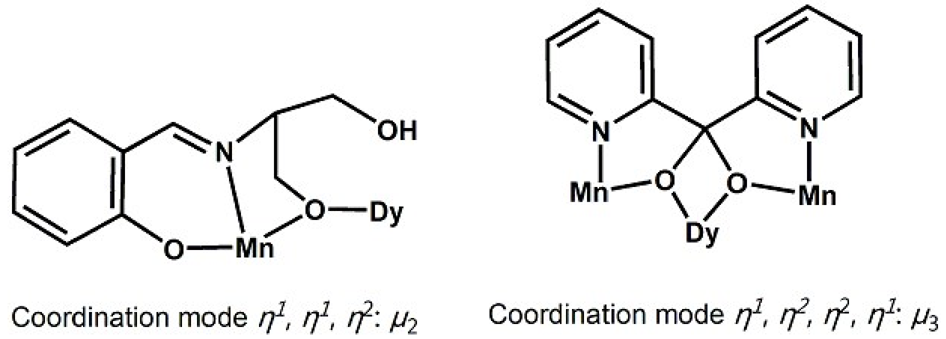

Scheme S1. The coordination modes of $(py)_2CO_2^{2-}$ and $(py)_2C(OH)O^-$ with metals for **1**.

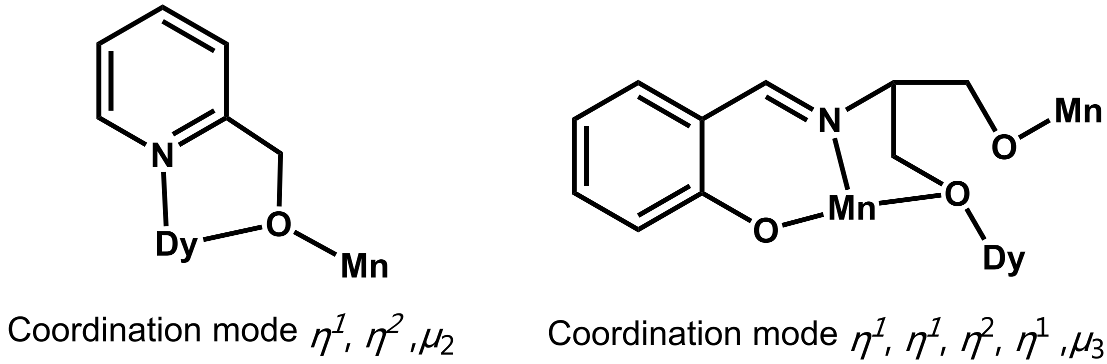

Scheme S2. The coordination modes of hmp^- and L^{3-} with metals for **2**.

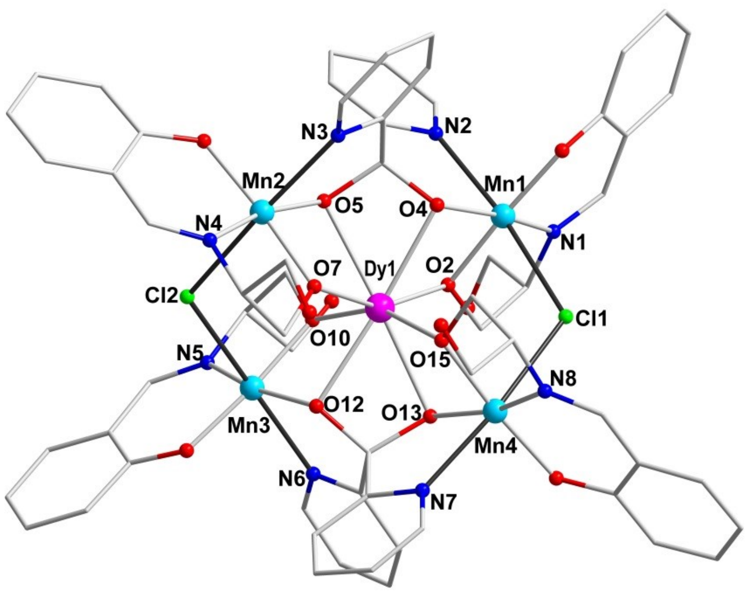

Fig. S1 Crystal structure of **1**. For clarity, the H atoms and solvent molecules were omitted. The thick black lines represent the Jahn-Teller axes of Mn^{III} ions in **1**.

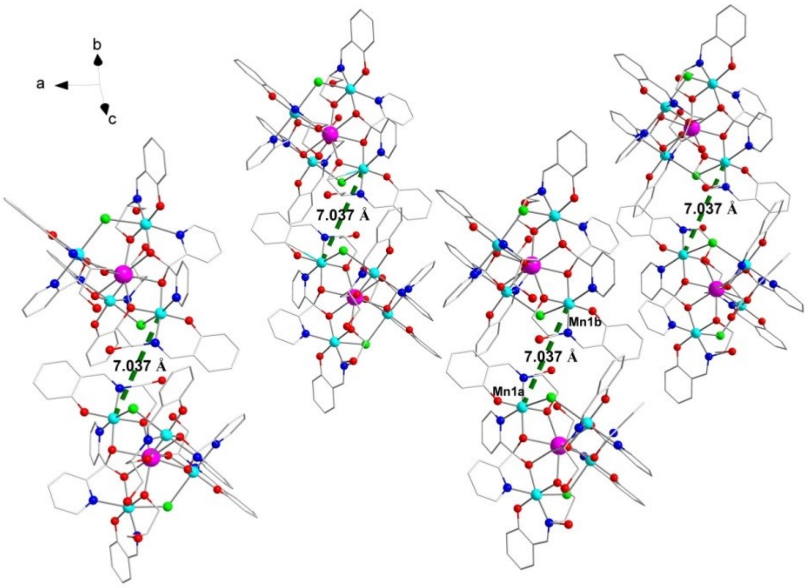

Fig. S2 The plot showing the distances of the metal ions between molecules of **1**.

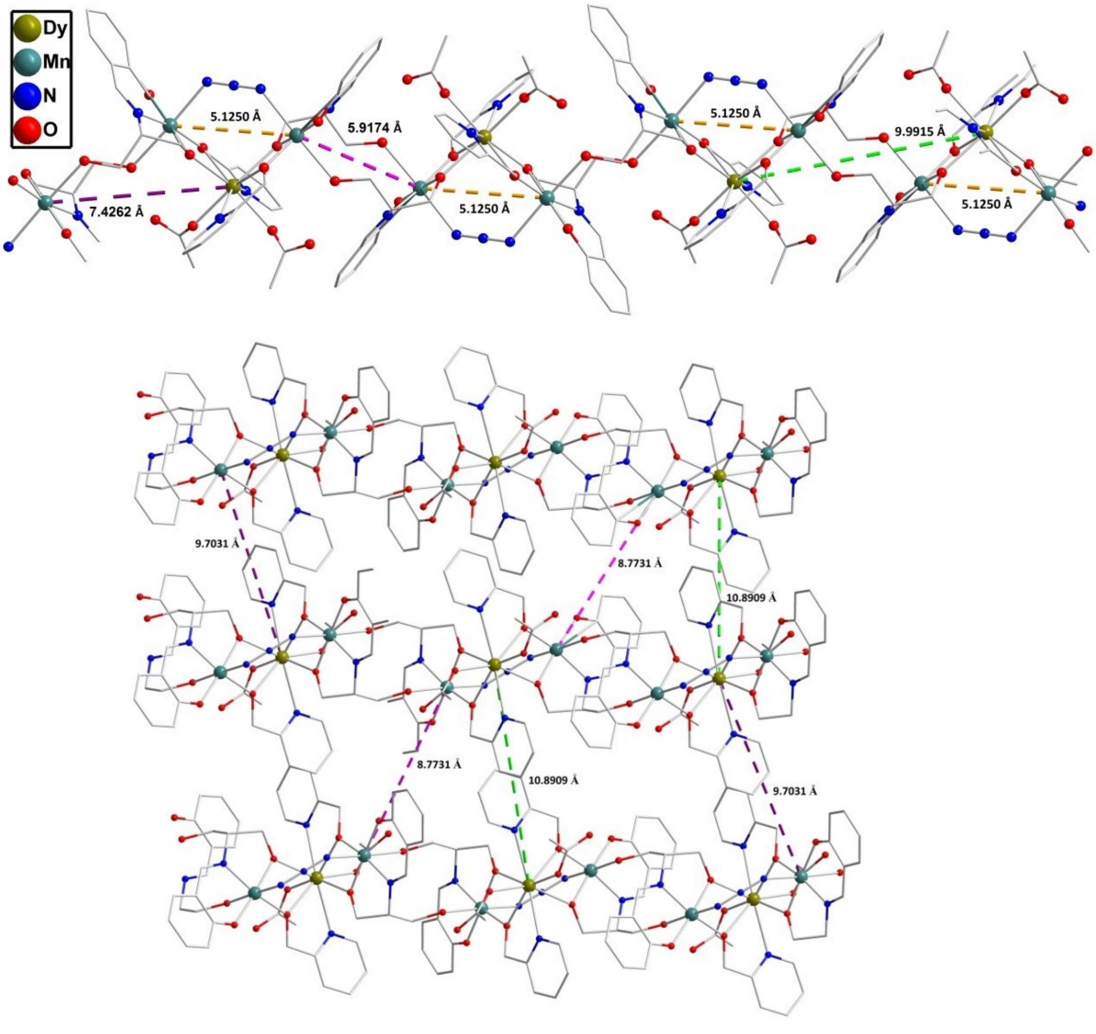

Fig. S3 The plots showing the distances of metal ions in the 1D chain (top) and the distances of metal ions between 1D chain (bottom) of the complex **2**.

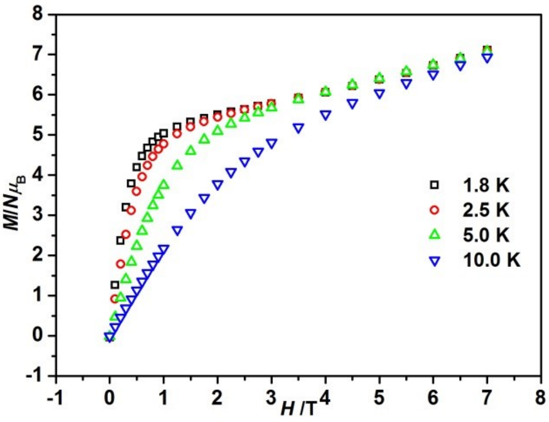

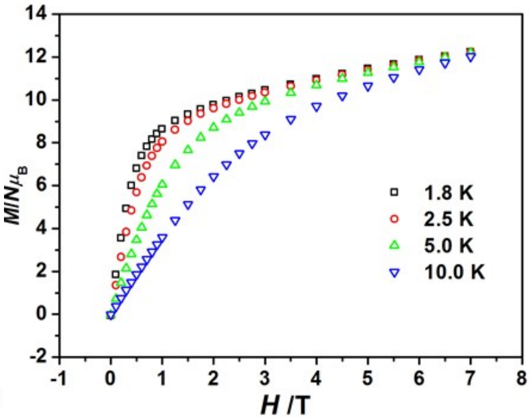

Fig. S4 The plots of the field dependence of the magnetization for **1** (left) and **2** (right) at different temperatures.

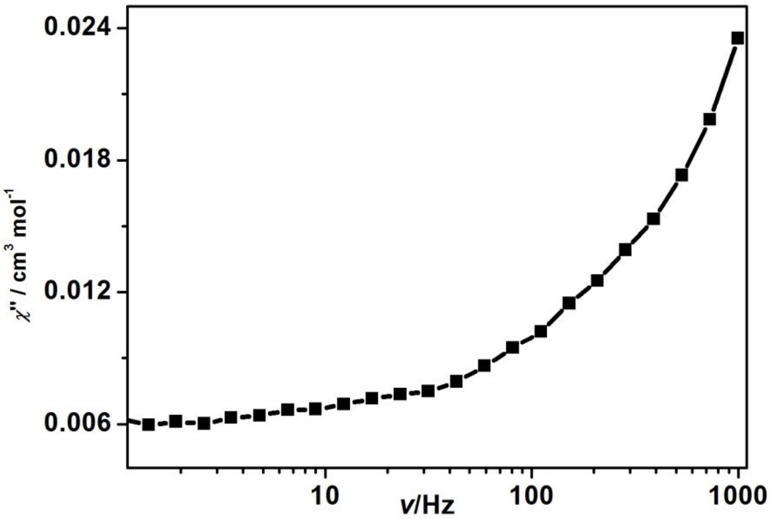

Fig. S5 Plot of χ'' *versus* frequencies (ν) for **1**collected under a 0 Oe dc field with the temperature 2.0 K.

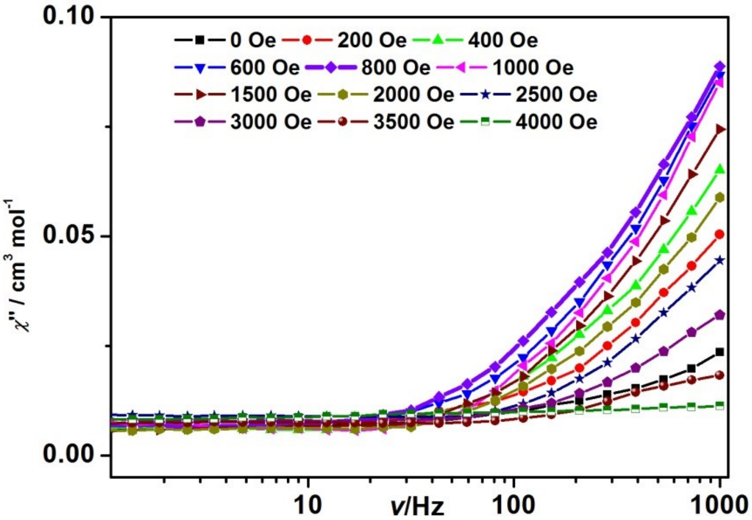

Fig. S6 Plots of out-of-phase (χ'') versus frequencies (ν) for **1** at 2.0 K with the applied dc field shown in plots.

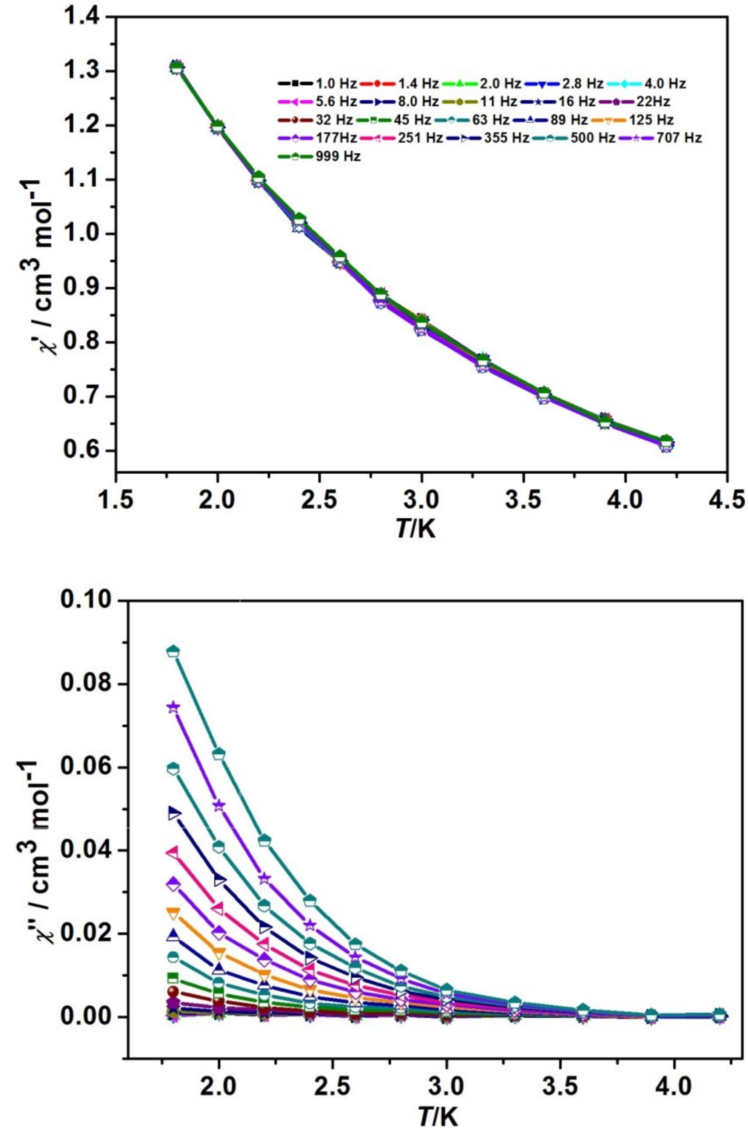

Fig. S7 Plots of χ' *versus* T (top) and χ'' *versus* temperatures (T) (bottom) for **1** under a dc field of 800 Oe.

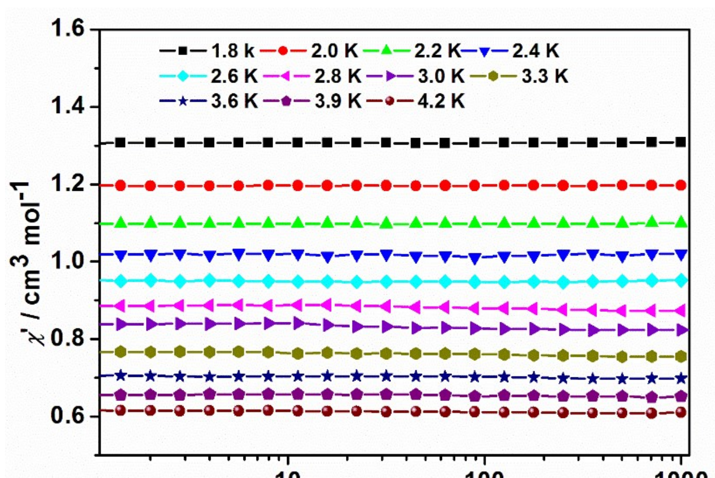

Fig. S8 Plots of χ' *versus* frequencies (v) for **1** under a dc field of 800 Oe.

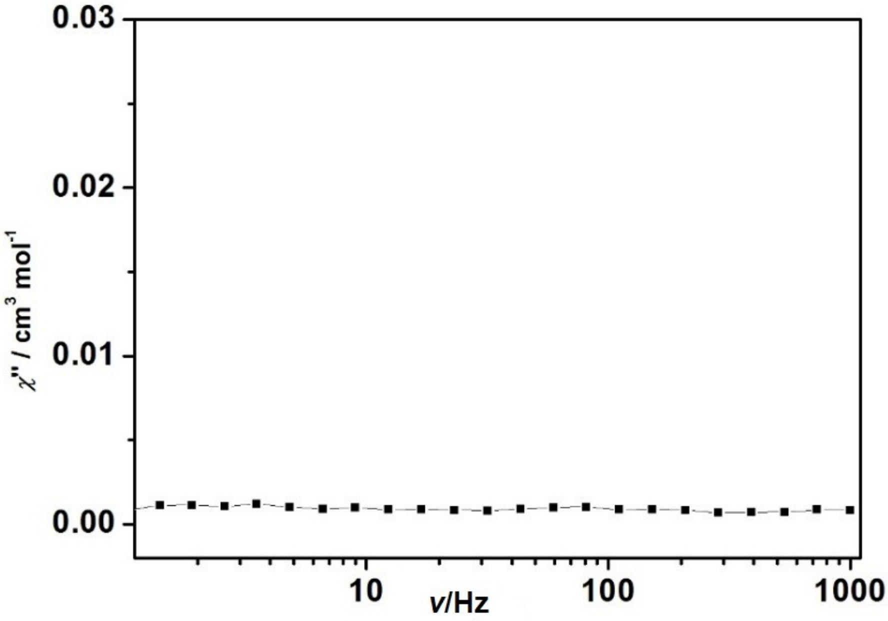

Fig. S9 Plot of χ'' *versus* frequencies (v) for **2** at 2.0 K under a 0 Oe dc field.

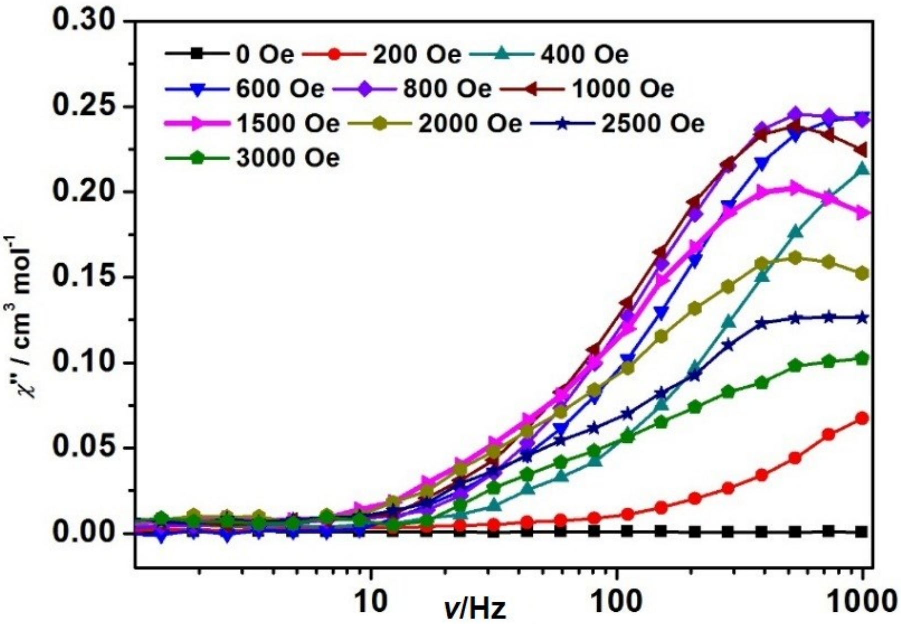

Fig. S10 Plots of χ'' *versus* frequencies (v) for **2** at 2.0 K with the applied dc field shown in plots.

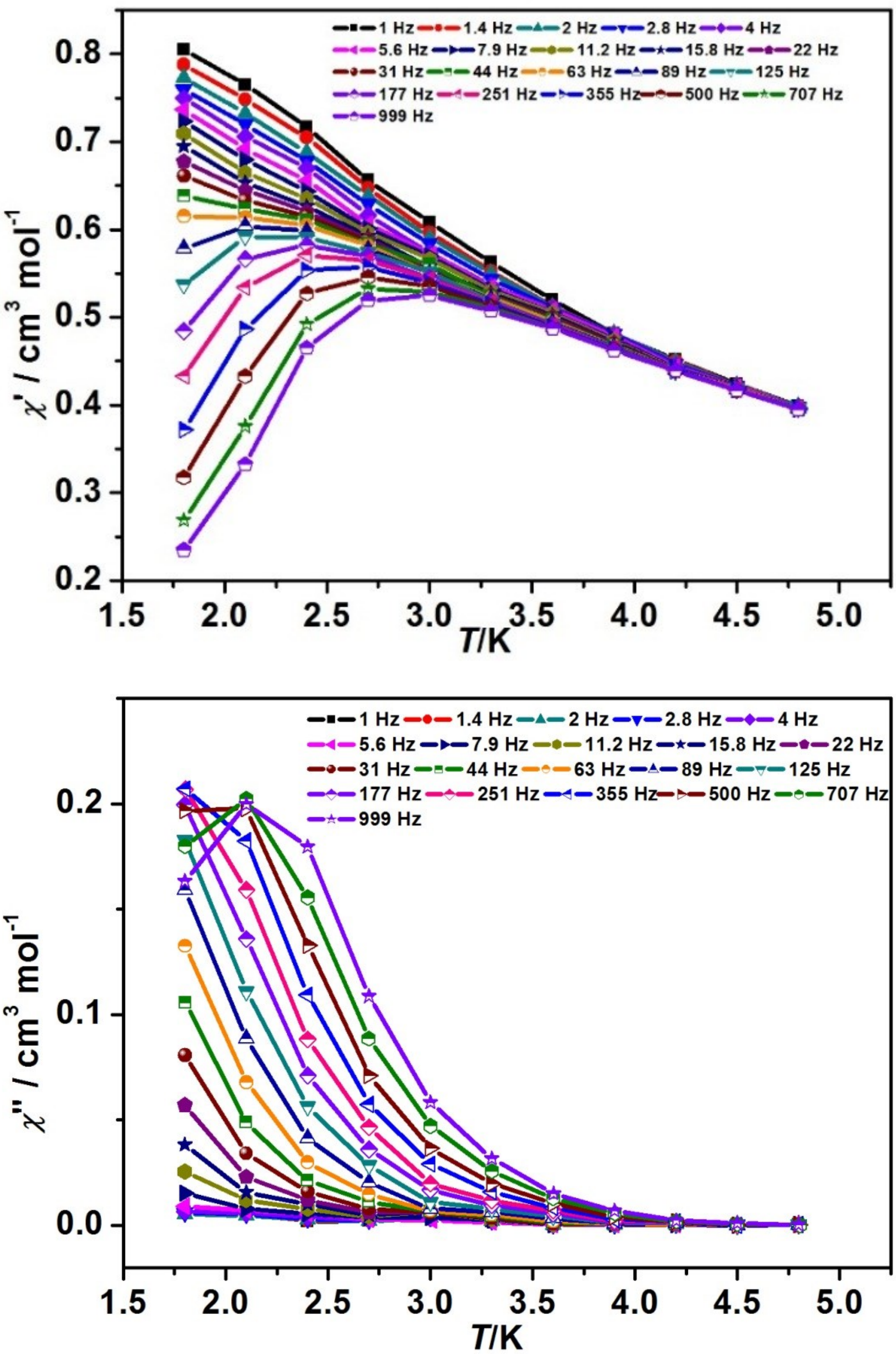

Fig. S11 Plots of χ' *versus* T (top) and χ'' *versus* temperatures (T) (bottom) for **2** under a dc field of 1500 Oe.

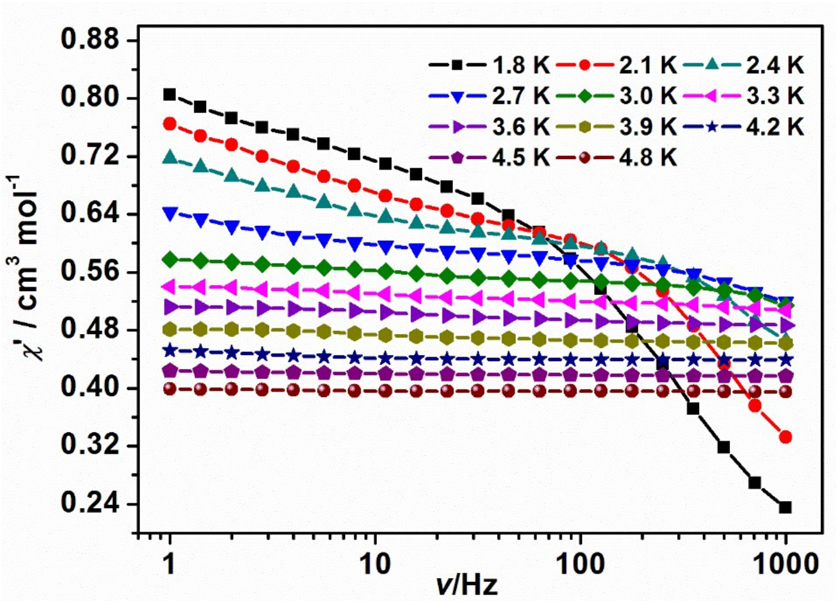

Fig. S12 Plots of χ' *versus* frequencies (v) for **2** under a dc field of 1500 Oe.

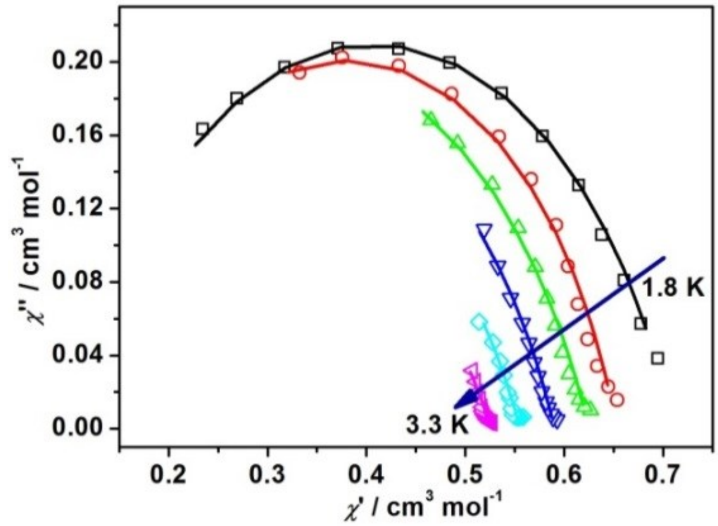

Fig. S13 Cole-Cole plots for complex **2** under 1500 Oe dc field. Solid lines show the fit of the data by employing the generalized single relaxation process Debye model.